Physical Modeling of the Upwind-Downwind Asymmetry in Microwave Return from the Sea Surface

Zaynab Guerraou, Sébastien Angelliaume, Charles-Antoine Guérin

PHYSICAL MODELING OF THE UPWIND-DOWNWIND ASYMMETRY IN MICROWAVE RETURN FROM THE SEA SURFACE

Zaynab Guerraou, Sébastien Angelliaume* and Charles-Antoine Guérin***

*ONERA, (The French Aerospace Lab), Electromagnetism and Radar Department, France.
**Université de Toulon, Aix Marseille Université, CNRS, IRD, MIO UM 110, La Garde, France

ABSTRACT

We report recent results on the investigation of upwind/downwind asymmetries in microwave return from the sea surface. We first provide a brief bibliographic synthesis of experimental trends observed for the upwind/downwind of the Normalized Radar Cross Section. This analysis enables the characterization of the asymmetries with respect to the radar geometry, the polarization channel, the sea state and the radar frequency. We consider various physical mechanisms which can account for upwind/downwind asymmetry and investigate in detail the role of unbalanced facet tilting. Using reference wind-wave tank experimental measurements, we design a probability distribution for the steep and asymmetric facet slopes and combine it with a Two-Scale Model. This allows recovering the trends of the asymmetries described in the literature.

Index Terms— Ocean microwave remote sensing, Two-Scale-Model, upwind/downind asymmetry

1. INTRODUCTION

The increasing number of airborne and spaceborne remote sensors operating in the microwave regime on the sea surface provides access to refined information on the surface signature and properties, both at global scale and at high spatial resolution. Sea surface wind vector is one of the key geophysical parameters in a wide range of meteorological and oceanographic applications. In this context, the sensitivity of the sea surface response to the wind direction and the related directional asymmetries are still not totally understood nor taken into account in physical models. The present work follows the earlier attempts to improve the understanding and modeling of these asymmetries. We first carry out (section 2) a thorough bibliographic survey aiming at characterizing the upwind/downwind asymmetry (UDA) as function of the radar geometry, polarization, wind speed and radar frequency. A second step consists in investigating the physical mechanisms that may be at the origin of these directional asymmetries (section 3). Our main point is that steep, asymmetric wave fronts are the dominant contributor to this phenomenon, at least in lower microwave bands. We therefore investigate the influence of the facet tilting mechanism through the use of a realistic description of large slopes and breaking events obtained from wind-wave tank experiments. The asymmetries obtained by combining these large slope distributions with a Two-Scale Model (TSM) are in qualitative agreement with the observations. Some possible perspectives are discussed in Section 4.

2. EXPERIMENTAL ANALYSIS

Over the last few decades, several Geophysical Model Functions (GMFs) have been established to relate the Normalized Radar Cross Section (NRCS) to the wind vector. For moderate incidence angles, these empirical models generally derive from a Fourier series expansion whose formulation for a given polarization and EM frequency is written as [1]

$$\sigma_0(U_{10},\theta,\phi) = a_0(U_{10},\theta,\phi)[1+\sum_{n=1}^{N} a_n(U_{10},\theta,\phi)cos(n\phi)] \quad (1)$$

where θ is the incidence angle, U_{10} the equivalent neutral wind speed measured at a 10-m height and ϕ the azimuth angle measured in the horizontal plane between the radar look and wind directions. This decomposition is usually truncated to the 2nd order. Table I summarizes the different GMFs considered in the present analysis and formulated following Eq. 1. Particular attention was paid to selecting reliable GMFs derived from data presenting a sufficient high signal-to-noise ratio. Currently, the majority of GMFs are established for co-polarized returns. However, an increasing interest is attributed to the study of cross-polarized data in alignment with the increasing full-polarization acquisition capacities. Our study is confined to HH and VV polarization. We note that cross-polarized data exhibit weaker directional asymmetries compared to co-polarized data [2].

Frequency	Spaceborn(SPA)/Airborn(Air)	Sensor and/or GMF name	Type	Polarization for GMF	Incidence angle	Wind speed	Reference
L	SPA	PALSAR	SAR	HH	[17°- 43°]	[0-20m/s]	[3]
	SPA	Aquarius	SCAT	HH-VV	29°, 38°, 56°	[0-20m/s]	[4,5]
	SPA	SMAP	SCAT	HH-VV	40°	[0-25m/s]	[6]
	AIR	PALS	SCAT	HH-VV	30°, 45°	[5-25m/s]	[7]
C	SPA	ERS-2(CMOD5.n)	SCAT	VV	[20°-60°]	[0-35m/s]	[8]
	AIR	IWRAP	Doppler	HH	[20°-60°]	[8-20m/s]	[9]
X	SPA	TS-X/TD-X(XMOD2)	SAR	VV	[20°-45°]	[0-20m/s]	[10]
	AIR	Masuko	SCAT	HH-VV	[0-70°]	[3.2-17.2m/s]	[11]
Ku	SPA	QuikSCAT (ku-2011)	SCAT	HH VV	46°, 54°	[0-35m/s]	[12]
Ka	AIR	Masuko	SCAT	HH-VV	[0°-70°]	[3.2-17.2m/s]	[11]
	Research Plateform	KaDPMod	Doppler radar	HH-VV	[25°-65°]	[3-18m/s]	[13]

Table 1: List of previously established GMFs based on data acquired by numerous sensors at various frequency bands, incidence angles and wind conditions.

The overall conclusions drawn from this bibliographic study can be summarized as follows:

- Polarimetric behavior: The UDA asymmetry is systematically higher in HH polarization compared to VV polarization. This suggests that the mechanisms at the origin of the UDA have more impact at HH than VV polarization. VV returns are proved to be mainly governed by Bragg-scattering, while HH returns are more sensitive to non-Bragg components that are likely to contribute to the UDA.
- Incidence angle behavior: The UDA increases with moderate incidence angles. At larger incidence angles, a decrease is often observed, yielding a non-monotonic variation of the UDA with a maximum occurring at a moderate incidence angle between 30 and 50 degrees. The position of this maximum depends on wind speed and radar frequency. It shifts towards smaller incidence angles as the wind speed increases. This non-monotonic variation is, however, not retrieved by some GMFs that predict a strictly increasing variation with incidence angle. Further investigation and improved accuracy is needed to confirm the behavior at large angles.
- Wind speed behavior: The various GMFs show a non-monotonic variation of the asymmetries with respect to wind speed, with a maximum occurring at moderate wind speeds at a position depending on the incidence angle and the radar frequency, shifting towards weaker wind speeds as the incidence angle increases.
- Frequency behavior: It is difficult to assert general conclusions on the frequency behavior based on GMFs derived from data acquired non-simultaneously by different sensors. However, the general trend seems to indicate an enhancement of the asymmetries as the radar frequency increases. This conclusion has been supported by the investigation of data acquired simultaneously at X and L bands in [14].

3. PHYSICAL MODELING OF THE UDA

Four physical mechanisms are repeatedly invoked in the literature in order to explain the upwind/downwind asymmetry:

- Tilt modulation: This purely geometrical mechanism consists in considering the asymmetry of large scale facets and assuming Gaussian statistics for small scales. Hence, the difference in reflectivity between the forward and the rear faces of the long waves is merely assigned to the local modification of the relative incidence angle by long wave slopes.

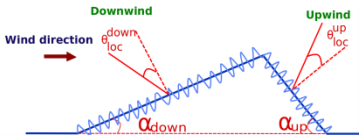

- Hydrodynamic modulation: In this scheme, the UDA is attributed to the modulation of the short waves riding on longer gravity waves. The ripples are more concentrated on the forward faces of the long waves compared to the rear faces. This modulation is commonly accounted for by introducing the so-called modulation transfer function based on non-linear wave-wave interactions.

- Non-Gaussian statistics: Aside from any Two-Scale argument, the UDA can also be accounted for by the deviation of the global sea surface slope statistics from the Normal distribution. Weakly non-Gaussian statistics are traditionally described by their cumulant expansions and based on measurements such as the Cox and Munk slope distribution [15]. However, weak deviations from the Normal distribution are insufficient to explain the magnitudes of the observed asymmetries.

- Non-Bragg scattering: Strong asymmetries are also attributed to various mechanisms related to the occurrence of breaking waves, foam, whitecaps etc., which cannot be described within the classical

framework of surface scattering theories. These include the wedge diffraction from sharp crests and steep waves as well as complex phenomena such as shadowing and multi-path scattering.

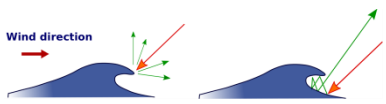

Hydrodynamic modulation has not been considered in the present work. Its contribution is thought to be significant in the upper microwave band (Ka band), but might not be sufficient to explain the asymmetries observed at lower frequency bands (X and C bands). Rigorous scattering from wedge-like profiles resorts to complex analytical and numerical calculations which are beyond the scope of this work. Our approach is focused on the study of the simple effect of tilt modulation which we propose to evaluate by combining a TSM with a realistic slope distribution of large slopes.

We use the GO-SSA model [16] whose formulation is given in Eq. 2. The model combines the geometrical optics (GO) for long waves and the Small-Slope Approximation (SSA1) [17] for short waves and allows straightforward modification of large slope distribution (denoted by P in Eq. 2).

$$\sigma_0^{GOSSA} = GO + \sigma_0^{SSA1} * \boldsymbol{P} \qquad (2)$$

The sea surface slope distribution has been established in the reference work by Cox and Munk [15] and later complemented by numerous subsequent measurements using optical and microwave sensors (e.g. [18,19]). However, limitations of optical measurement techniques and inversion methods usually do not allow accounting for the large slopes associated to steep asymmetric waves and breaking events. Even though the probability of occurrence of these events is relatively small, their potential contribution to the polarized asymmetries is significant. Furthermore, the distribution of filtered slopes (i.e pertaining to some ranges of wave scales) which is needed in the TSM is in general unknown. Today, there is still a lack of accurate measurements or estimations of sea surface slopes at all scales, including higher slopes from steep fronts and breaking waves, among others. In this study we used an experimental one-dimensional slope distribution inferred from measurements carried out in the large Marseille-Luminy wind-wave facility using an imaging technique described in [20]. During the experiment, several regimes corresponding to a variety of wind and fetch conditions have been identified. We selected the case with the strongest wind and fetch parameters (8 m/s and 13 m, respectively) corresponding to a gravity wave regime (regime 4 in [20]). The corresponding slope distribution (along the wind axis) is shown in Fig. 1 together with the reference Gaussian distribution. A significant deviation from the latter is observed at large wave slopes, with a marked asymmetry and a faster fall-off for positive slopes (downwind facets) and a slower decay for negative slopes (upwind facets).

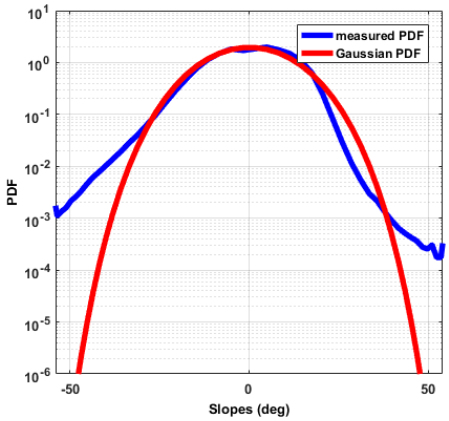

Figure 1: Slope distribution of regime 4 in [18] in semi-logarithmic scale (blue). Superimposed (red) is the Gaussian distribution with the same mean and variance.

Even though this distribution corresponds to a particular wind and fetch, we assume its normalized shape is universal, by virtue of the self-similarity properties of near-breaking short gravity wind waves [21] and can thus be applied to any wave scale in the gravity wave regime. In the absence of any other knowledge, we use this universal distribution shape to form an asymmetric facet-slope distribution along the wind axis, and complement it with a Gaussian distribution in the crosswind direction (discarding at this stage purely three-dimensional effects such as horseshoe patterns). The mean square slopes (mss) along the x- and y-axis are adapted to the small-scale cut-off of the TSM (a few radar wavelengths). An estimation of the filtered mss at X-band can be obtained using the Cox and Munk "slick" distribution [15] (with a cut-off at about 30 cm, that is 10 radar wavelengths). For the facet slope distribution at L band we use the airborne measurements described in [19] providing the slope distribution of 1-2 m segments at the sea surface (that is about 10 radar wavelengths). An example of the UDA modelled at X-band using the combination of the GO-SSA model and Elfouhaily spectrum [22] with the asymmetric facet slope distribution is shown in Fig. 2. Unlike the NRCS obtained assuming Gaussian slope statistics, the NRCS exhibits a pronounced asymmetry. The non-monotonic incidence angle behavior is retrieved with a maximum at a moderate incidence angle laying between 30° and 40°. The polarimetric behavior with a larger asymmetry at HH polarization compared to the VV counterpart is also recovered.

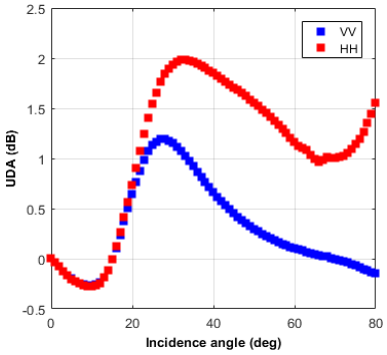

Figure 2: UDA obtained using the GO-SSA model combined with Elfouhaily spectrum and the experimental slope distribution, U_{10} =9.5 m/s.

5. CONCLUSION AND PERSPECTIVES

In this paper, a synthesis of experimental analysis of directional asymmetries as derived from GMFs in the literature is provided. A theoretical investigation of the UDA is then undertaken by combining a TSM with experimental slope distributions obtained from wind-wave tank measurements. The inferred UDA features at X band are in qualitative agreement with the observations in terms of incidence angle and polarization behaviors. Further statistical slope measurements at various wind conditions are needed in order to probe the UDA variation with respect to wind speed. Moreover, the results are very sensitive to the mean square slope estimations used to adapt the laboratory slope distribution to sea surface conditions. More accurate measurements of the sea surface mss are required in order to perform reliable and quantitative frequency analysis. Furthermore, the model used in our simulations does not incorporate hydrodynamic modulation whose contribution might be substantial, especially at higher frequency bands. Previous studies on the upwind/downwind emission asymmetry from the sea surface [23,24] suggest that the sole long wave tilting is indeed not the only relevant mechanism to consider. Further studies are needed to accurately account for this hydrodynamic modulation and evaluate its contribution to the asymmetry.

5. REFERENCES

[1] Hersbach, H., A. Stoffelen, and S. de Haan (2007), An improved C-band scatterometer ocean geophysical model function: CMOD5, J. Geophys. Res., 112, C03006.

[2] Z. Guerraou, S. Angelliaume, L. Rosenberg and C. A. Guérin, "Investigation of Azimuthal Variations From X-Band Medium Grazing-Angle Sea Clutter," in IEEE Transactions on Geoscience and Remote Sensing, vol. 54, no. 10, pp. 6110-6118, Oct. 2016.

[3] O. Isoguchi and M. Shimada. An l-band ocean geophysical model function derived from palsar. IEEE Trans. Geosc. Rem. Sens., 47(7) :1925–1936, July 2009.

[4] S. H. Yueh, W. Tang, A. G. Fore, G. Neumann, A. Hayashi, A. Freedman, J. Chaubell, and G. S. E. Lagerloef. L-band passive and active microwave geophysical model functions of ocean surface winds and applications to Aquarius retrieval. IEEE Trans. Geosc. Rem. Sens., 51(9) :4619–4632, Sept 2013.

[5] S. H. Yueh,W. Tang, A.G. Fore, A.K. Hayashi, Y.T. Song, and G. Lagerloef. Aquarius geophysical model function and combined active passive algorithm for ocean surface salinity and wind retrieval. J. Geophys. Res.: Oceans, 119(8) :5360–5379, 2014.

[6] X. Zhou, J. Chong, X. Yang, W. Li, and X. Guo. Ocean surface wind retrieval using SMAP L-band sar. IEEE Journal of Selected Topics in Applied Earth Observations and Remote Sensing, 10(1) :65–74, Jan 2017.

[7] H. Yueh, S. J. Dinardo, A. G. Fore, and F. K. Li. Passive and active l-band microwave observations and modeling of ocean surface winds. IEEE Trans. Geosc. Rem. Sens., 48(8) :3087–3100, Aug 2010.

[8] H. Hersbach. CMOD5.N : A C-band geophysical model function for equivalent neutral wind., April 2008.

[9] J.W. Sapp, S. O. Alsweiss, Z. Jelenak, P. S. Chang, S. J. Frasier, and J. Carswell. Airborne copolarization and cross-polarization observations of the ocean-surface NRCS at C-band. IEEE Trans. Geosc. Rem. Sens., 54(10) :5975–5992,Oct 2016.

[10] F. Nirchio and S Venafra. XMOD2- an improved geophysical model function to retrieve sea surface wind fields from cosmo-sky med x-band data. European Journal of Remote Sensing, 46(1) :583–595, 2013. doi : 10.5721/EuJRS20134634.

[11] Harunobu Masuko, Ken'ichi Okamoto, Masanobu Shimada, and Shuntaro Niwa. Measurement of microwave backscattering signatures of the ocean surface using x band and ka band airborne scatterometers. J. Geophys. Res.: Oceans, 91 (C11) :13065–13083, 1986. ISSN 2156-2202.

[12] Lucrezia Ricciardulli and Frank J.Wentz. A scatterometer geophysical model function for climate-quality winds : Quikscat ku-2011. Journal of Atmospheric and Oceanic Technology, 32(10), Oct 2015

[13] Y. Y. Yurovsky, V. N. Kudryavtsev, S. A. Grodsky, and B. Chapron. Ka-band dual copolarized empirical model for the sea surface radar cross section. IEEE Trans. Geosc. Rem. Sens., 55(3) :1629–1647, March 2017.

[14] Z.Guerraou, S. Angelliaume, and C. A.Guérin. Multifrequency analysis of radar sea clutter directional asymmetries. In 2017 IEEE IGARSS July 2017.

[15] C. Cox and W. Munk. Measurement of the roughness of the sea surface from photographs of the sun's glitter. J. Opt. Soc. Am., 44(11) :838–850, Nov 1954.

[16] G. Soriano and C. A. Guerin, "A Cutoff Invariant Two-Scale Model in Electromagnetic Scattering From Sea Surfaces," in IEEE Geoscience and Remote Sensing Letters, vol. 5, no. 2, pp. 199-203, April 2008.

[17] A. G. Voronovich. Small-slope approximation in wave scattering from rough surfaces. Journal of Experimental and Theoretical Physics, 62(1) : 65–70, 1985.

[18] Bréon, F., and N. Henriot (2006), Spaceborne observations of ocean glint reflectance and modeling of wave slope distributions, J. Geophys. Res., 111, C06005

[19] Vandemark, D., B. Chapron, J. Sun, G. Crescenti, and H. Graber (2004), Ocean wave slope observations using radar backscatter and laser altimeters, J. Phys. Oceanogr., 34, 2825–2842.

[20] G.Caulliez and Charles-Antoine Guérin. Higher-order statistical analysis of short wind wave fields. J. Geophys. Res.: Oceans, 117(C6): C06002, 2012.

[21] G. Caulliez. Self-similarity of near-breaking short gravity wind waves. Physics of Fluids AIP Publishing, 2002.

[22] T. Elfouhaily, B. Chapron, K. Katsaros, and D. Vandemark. A unified directional spectrum for long and short wind-drivenwaves. Journal of Geophysical Research, 102(C7) : 15781–15796, 1997.

[23] V. G. Irisov, "Azimuthal variations of the microwave radiation from a slightly non-Gaussian sea surface," Radio Sci., vol. 53, pp. 65–82, 2000.

[24] J. T. Johnson and Yongyao Cai, "A theoretical study of sea surface up/down wind brightness temperature differences," in IEEE Transactions on Geoscience and Remote Sensing, vol. 40, no. 1, pp. 66-78, Jan 2002.